

The calibration system of the Muon $g-2$ experiment

A. Driutti^{a,b,*}, A. Basti^c, F. Bedeschi^c, G. Cantatore^{d,a}, D. Cauz^{b,a}, G. Corradi^e, S. Dabagov^{e,f,g}, S. Di Falco^c, G. Di Sciascio^h, R. Di Stefano^{i,j}, S. Donati^c, O. Escalante^{j,k}, C. Ferrari^{c,l}, A. Fioretti^{c,l}, C. Gabbanini^{c,l}, A. Gioiosa^{h,m}, D. Hampai^e, M. Iacovacci^{j,k}, M. Incagli^c, M. Karuza^{n,l}, A. Lusiani^{c,o}, F. Marignetti^{i,j}, S. Mastroianni^j, D. Moricciani^h, A. Nath^j, G. Pauletta^{b,a}, G.M. Piacentino^{h,m}, N. Raha^c, L. Santi^{b,a}, M. Smith^c, M. Sorbara^h, G. Venanzoni^c

^a INFN, Sezione di Trieste e G.C. di Udine, Trieste, Italy

^b Università di Udine, Udine, Italy

^c INFN, Sezione di Pisa, Pisa, Italy

^d Università di Trieste, Trieste, Italy

^e Laboratori Nazionali Frascati dell'INFN, Frascati, Italy

^f PN Lebedev Physical Institute, Moscow, Russia

^g NR Nuclear University MEPhI MEPhI, Moscow, Russia

^h INFN, Sezione di Roma Tor Vergata, Roma, Italy

ⁱ Università di Cassino, Cassino, Italy

^j INFN, Sezione di Napoli, Napoli, Italy

^k Università di Napoli, Napoli, Italy

^l Istituto Nazionale di Ottica del C.N.R., UOS Pisa, Pisa, Italy

^m Università del Molise, Pesche, Italy

ⁿ University of Rijeka, Rijeka, Croatia

^o Scuola Normale Superiore, Pisa, Italy

ARTICLE INFO

Keywords:

Electromagnetic calorimeter

Laser system

Muon $g-2$

Calibration methods

Optics

ABSTRACT

The Muon $g-2$ experiment at Fermilab (E989) plans to measure the muon anomalous magnetic moment to a precision of 140 parts per billion (ppb), which corresponds to a total uncertainty of 1.6×10^{-10} . To achieve this level of precision the experiment must detect more than 1.8×10^{11} decay positrons by using the 24 calorimeters distributed around the muon storage ring. Each calorimeter consists of 54 PbF_2 crystals read out by SiPMs. The response of each of the 1296 channels must be calibrated and monitored to keep uncertainties due to gain fluctuations at the sub-per mil level in the time interval corresponding to one beam fill (700 μs) and at the sub-percent level on longer time scales. These requirements are much more demanding than those needed by most high energy physics experiments. This paper presents a novel laser-based calibration system that distributes light to all calorimeter cells, while allowing one to correct for laser intensity fluctuations and to monitor the distribution chain stability at unprecedented levels of accuracy. Results on the system performance during the first few months of stored muon operation in 2018 are also presented.

* Corresponding author at: Università di Udine, Udine, Italy.

E-mail address: Anna.Driutti@ts.infn.it (A. Driutti).

1. Introduction

The muon anomaly, is a dimensionless quantity computed as $a_\mu = (g_\mu - 2)/2$. The factor g_μ is a proportionality constant that relates the magnetic dipole moment of the muon and its spin, and it is expected to be 2 for spin 1/2 particles at the tree level in the quantum electrodynamics theory. In the Standard Model, the quantum corrections from electrodynamic (a_μ^{QED}), electroweak (a_μ^{EW}) and hadronic (a_μ^{Had}) interactions are such that g_μ is greater than 2, and the theoretical expectation of a_μ^{SM} is

$$a_\mu^{\text{SM}} = a_\mu^{\text{QED}} + a_\mu^{\text{EW}} + a_\mu^{\text{Had}} = (116591802 \pm 49) \times 10^{-11} \quad [1]. \quad (1)$$

The theoretical value a_μ^{SM} in Eq. (1) is known with a precision of 420 ppb and its uncertainty is dominated by the hadronic term. A recent re-evaluation of a_μ^{Had} resulted in a total value of the anomalous magnetic moment of the muon of

$$a_\mu^{\text{SM}} = (116591820.5 \pm 35.6) \times 10^{-11} \quad [2]. \quad (2)$$

The comparison of a_μ^{SM} with the experimental measurement allows for a stringent test of the Standard Model.

The most recent precise experimental measurement of the muon anomalous magnetic moment obtained

$$a_\mu^{\text{E821}} = (116592089 \pm 63) \times 10^{-11} \quad [3]. \quad (3)$$

This value is the result of the E821 experiment performed at the Brookhaven National Laboratory (BNL) and it is about 3.6 standard deviations (3.6σ) larger than the expected a_μ^{SM} reported in Eq. (1). To confirm that the discrepancy is due to new physics, the Fermilab $g-2$ experiment (E989) aims to measure a_μ with a precision of 140 ppb. If the E989-measurement would yield the same mean value for a_μ as that in Eq. (3), and improvements on the theoretical uncertainty are considered (*i.e.*, Eq. (2)), the significance of the deviation from the SM prediction could reach 7σ [2].

To achieve the challenging goal of reducing by a factor 4 the uncertainty on the experimental measurement, the E989 collaboration is planned to use the FNAL accelerator complex for delivering 21 times more muons into the same magnetic storage ring of E821 equipped with improved detectors [4]. In particular, the experiment will be instrumented with 24 new electromagnetic calorimeters, calibrated by a sophisticated laser calibration system.

2. The Fermilab Muon $g-2$ experiment

The experimental technique is based on the injection of a 3.1 GeV/ c beam of polarized anti-muons inside a 1.4 T magnetic storage ring. In the presence of a magnetic field (\vec{B}) the muon anomaly introduces an anomalous precession frequency that could be written as:

$$\omega_a = a_\mu \frac{e}{m} B \quad (4)$$

where e is the electron charge and m is the mass of the muon. Eq. (4) holds only for muons with magic momentum of 3.1 GeV/ c , for which, in first approximation, the contributions from the electric field term to ω_a cancels out and, the value of a_μ can be determinate by measuring B , the strength of the magnetic field, and ω_a .

The magnetic field is measured directly by nuclear magnetic resonance (NMR) probes, while ω_a is obtained by detecting the positrons that decay from the stored muons.

2.1. Measurement of the anomalous precession frequency with the calorimeters

Anti-muons, while circulating inside the ring, decay into positrons and neutrinos. Since the decay positrons do not have enough energy to keep the anti-muon trajectory, they curl inwards where 24 electromagnetic calorimeter stations are placed to detect them. Each calorimeter

Table 1

Contributions of various factors to the total systematic uncertainty of the anomalous precession frequency ω_a measurement.

Category	E989 Improvements	Goal [ppb]	E821 [ppb]
Gain stability	Laser calibration, low-energy threshold	20	120
Pileup	Low-energy samples, calorimeter segmentation	40	80
Lost muons CBO ¹	Collimation in ring, Higher n value (frequency), match of beamline to ring	20	90
Electric field and pitch	Tracker, storage ring simulations	< 30	50
Total	Quadrature sum	70	180

¹ Coherent Betatron Oscillation.

is composed of 54 lead-fluoride crystals read out by large-area silicon-photomultiplier (SiPM) arrays for a total of 1296 channels around the ring [5,6]. The high energy positrons are preferentially emitted with momentum aligned to the muon spin and their emission direction is modulated by ω_a . Then, the anti-muon precession can be extracted by counting the number of decayed positrons with an energy above a defined threshold as a function of the time. The calorimeters are designed to measure the hit times and energy of these decay positrons with time resolution better than 100 ps for positrons with energy greater than 100 MeV and with energy resolution better than 5% for reconstructed positron energy higher than 2 GeV [4].

The systematic uncertainty budget for the ω_a measurement is 70 ppb, *i.e.*, half of the total uncertainty expected for the E989 experiment [4]. Details on the systematic uncertainties expected on the ω_a measurement, are show in Table 1.

The first two categories are directly related to the calorimeters, while the last three are connected to improvements of other detectors. The systematic uncertainty for the ω_a measurement performed by the E821 experiment are reported in the last column. The biggest improvement expected is from the laser calibration system.

3. The laser calibration system for the calorimeters

The laser calibration system provides absolute calibration, gain stability and time synchronization for all the 1296 channels of the calorimeters [7].

The system is schematically drawn in Fig. 1. A custom laser control board (LCB) [8] is interfaced to an 8-channel multi-laser driver (PDL828 Sepia II) to trigger 6 laser heads (LDH-P-C-405 M by PicoQuant) simultaneously. Each laser head provides up to 1 nJ of pulses 700 ps wide at a wavelength of 405 nm. The light of each pulse is split by a 70:30 beam splitter. The part with 70% of the light is further divided into 4 equal parts by means of additional 50:50 beam splitters. Each of the four resulting beams is transported to one of the calorimeters in the ring using 25 m-long quartz optical fibers. In the calorimeter stations this light is expanded by a diffuser and delivered into a fiber bundle which takes the light to each calorimeter crystals by means of a panel with optical prisms located in front of the calorimeter. The remaining 30% of the laser light is directed to a Source Monitor (SM) which is used to measure pulse-by-pulse the intensity of the laser. The SM is contained inside a solid aluminum case and consists of an integrating sphere, 2 large area PIN diodes and a PMT. The incoming laser light is distributed among the photo-detectors by the integrating sphere, the two PINs provide fast precise monitoring, while the PMT, which is also exposed to an Am/NaI “light pulser” is used for slow absolute calibration [9]. The signals from the SMs photo-detectors are digitized by custom electronics modules [10,11] and acquired using μ TCA-based waveform digitizers [12]. Part of the light entering the SM is captured by a fiber minibundle and is used as reference signal by the Local

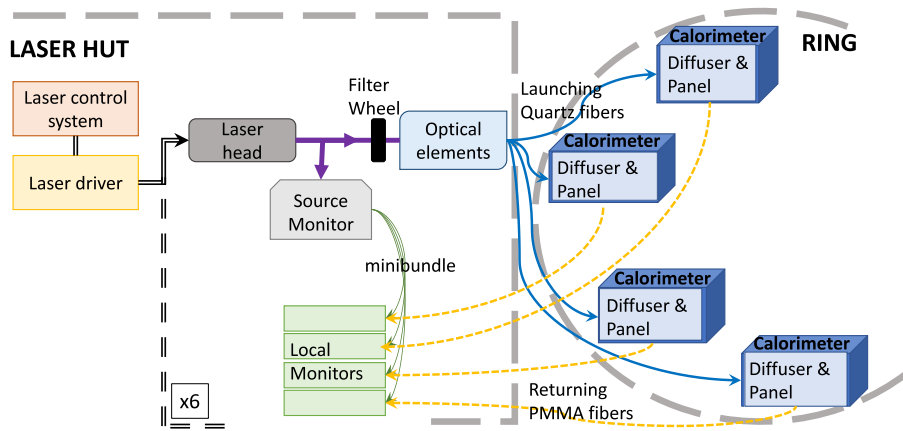


Fig. 1. Schematic drawing of the laser calibration system. The laser driver controls 6 laser heads each of them calibrates 4 calorimeters. For simplicity only the distribution chain for one laser head is depicted, the other 5 are identical. Most of the system is contained inside a room near the storage ring called laser hut. See text for the description of the elements.

Monitors (LMs). Each LM consists of a PMT which collects the light from the SM and the light from the diffuser in the calorimeter which is transported back by a PMMA fiber. The stability of the distribution system is monitored by comparing the amount of light from the two sources.

The laser calibration system is connected to the experiment clock, control and command (CCC) system through the laser control board, which triggers the light pulses with pre-configured patterns designed for calibrations and calorimeter performances studies during and between data-taking [8]. Anti-muons are injected into the storage ring in trains of bunches separated by 200 or 1000 ms. Each bunch consists of 8 fills, 700 μs time long, in the course of which the anti-muons decay. When the CCC issues the start of the muon fill, the LCB triggers the laser driver to pulse two times: after 5 μs (begin-of-fill pulse, BOF) and after 690 μs (end-of-fill pulse, EOF). To monitor the gain stability during the fill (in-fill), the LCB triggers the laser driver to pulse 2 times between the BOF and the EOF pulses once every 9 fills. These two pulses, called in-fill pulses, are separated by 200 μs and are moved forward by 2.5 μs each time, so that at the end by combining the muon fills with in-fill pulses the entire time interval from the BOF and the EOF has been scanned by laser pulses. During the 10 ms between fills (laser fills) the CCC issues a new trigger to the LCB, which triggers the laser pulses with the out-of-fill sequence: four pulses separated by 200 μs .

Offline, the BOF and the EOF pulses are used as a quality check that the whole fill was correctly acquired and for time synchronization of the crystals. The in-fill laser pulses are used to monitor the gain stability during the fill, while the out-of-fill sequence is used to monitor the long term gain stability.

3.1. Performance

Fig. 2 shows a preliminary example of the average relative gain of a calorimeter (black dots) measured using the in-fill laser pulses during the first 400 μs of the fill after injection. The biggest effect ($\sim 3\%$ drop) is noticeable shortly after injection where the large flux of particle entering into the storage ring saturates the calorimeters. About 30 μs after beam injection the calorimeter gain is quite stable. The square points show the corresponding laser light fluctuations measured by the monitors of the laser calibration system.

To reach the precision required by the experiment, from the measurement shown in Fig. 2, it is necessary to correct for the gain variation caused by the beam pulses that immediately preceded the laser pulse on a time scale of several tens of nanoseconds (double-pulses). The effect on the gain due to these double-pulses is estimated using the laser calibration system by sending the light of two lasers into the same four calorimeters, when there is no beam. This can be achieved by deviating the light of the odd (even) laser heads by raising a mirror in front of

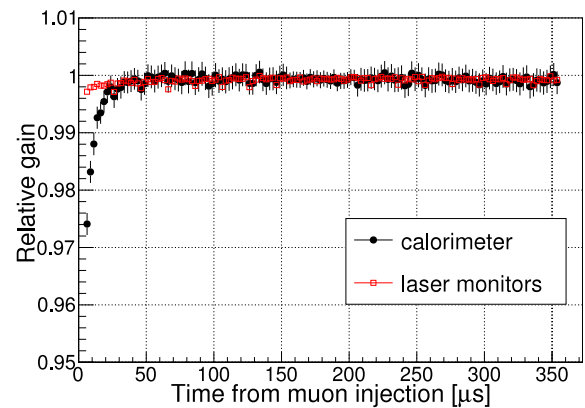


Fig. 2. Preliminary example of the average relative gain of a calorimeter (black dots) during the first 400 μs after muon injection measured by the laser calibration system. The gain function is not corrected for the fluctuations of the laser light (open square points) measured by the laser calibration system monitors.

them. With this new hardware configuration it is possible to illuminate the calorimeters with two laser pulses distant only few nanoseconds in time. A preliminary example of the result of this study is shown in Fig. 3. The gain of the second pulse is reduced of about 6% when there is a pulse about 4 ns before, and the effect vanishes when there are about 70 ns between the pulses.

This measurement is important to reduce the systematic uncertainty related to the pileup (positrons that hit the same calorimeter crystal at the same time), which played a major role in the previous experiment [13] and is expected to not exceed 20 ppb in E989 (see Table 1). Moreover, the same hardware setup, in which two laser are firing into the same four calorimeters, is used to evaluate the microsecond level variation due to the power supply system.

The SiPMs used as photo-detectors by the E989-calorimeters, are very sensitive to temperature and bias voltage variation. These effects result in gain variations which occur in a time scale much longer than the 700 μs muon fills. To correct for this long-term drift in the calorimeters' gain, the pulses of the out-of-fill sequence are used. The technique has been tested with an electron beam in test beam facilities [6,8].

4. Conclusion

This paper describes the architecture and the preliminary performance results of the novel laser-based calibration system for the calorimeters of the Muon $g-2$ experiment at Fermilab. The design of the system was driven by the calorimeters requirement of a gain stability at

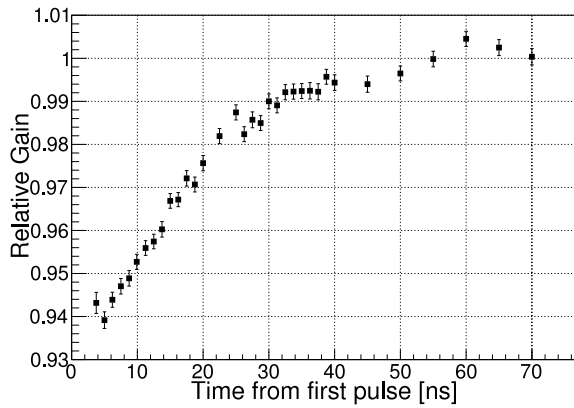


Fig. 3. Preliminary example of relative gain variation due to the presence of a first pulse close in time to the second.

the sub-per-mil level within a fill to measure the anomalous precession frequency ω_a with a systematic uncertainty of 70 ppb. To achieve this goal the calibration system uses 6 laser heads to calibrate and monitor each of the 1296 calorimeter channels individually, and comprises two kinds of monitors (the source monitors and the local monitors) to control the fluctuations introduced by the laser light and the distribution chain. The laser calibration system is connected to the main data-acquisition of the experiment through the custom made laser control board which triggers the laser heads to fire with defined sequences. These sequences of pulses are studied ad hoc to monitor and correct for the gain variations in the calorimeters. The two preliminary results from the first few months of the 2018 stored muon operation presented in this

paper show that the laser calibration system is successful in delivering the performance required by the experiment.

Acknowledgments

This research was supported by Istituto Nazionale di Fisica Nucleare (Italy), by Fermi Research Alliance, LLC under Contract No. DE-AC02-07CH11359 with the United States Department of Energy, and by the EU Horizon 2020 Research and Innovation Program under the Marie Skłodowska-Curie grant agreements No. 690385 (MUSE), No. 734303 (NEWS).

References

- [1] M. Davier, A. Hoecker, B. Malaescu, Z. Zhang, *Eur. Phys. J. C* 71 (2011) 1515; *Eur. Phys. J. C* 72 (2012) 1874 (erratum).
- [2] A. Keshavarzi, D. Nomura, T. Teubner, [arXiv:1802.02995](https://arxiv.org/abs/1802.02995) [hep-ph].
- [3] G.W. Bennett, et al., *Phys. Rev. D* 73 (2006) 072003.
- [4] J. Grange, et al., [Muon $g-2$ Collaboration] (2015) [arXiv:1501.06858](https://arxiv.org/abs/1501.06858) [physics.ins-det].
- [5] J. Kaspar, et al., *J. Instrum.* 12 (01) (2017) P01009.
- [6] A.T. Fienberg, et al., *Nucl. Instrum. Methods A* 783 (2015) 12.
- [7] A. Anastasi, et al., Electron beam test of key elements of the laser-based calibration system for the Muon $g-2$ experiment, *Nucl. Instrum. Methods A* 842 (2017) 86.
- [8] A. Anastasi, et al., Submitted to Elsevier (2017).
- [9] G. Pauletta, et al., *Open Access House Sci. Technol.* 1 (1) (2017).
- [10] M. Iacovacci, These Proceedings.
- [11] S. Mastroianni, These Proceedings.
- [12] D.A. Sweigart, [Muon $g-2$ Collaboration], PoS ICHEP 2016, 2016, p. 845.
- [13] J. Kaspar, [Fermilab E989 Collaboration], *Nucl. Part. Phys. Proc.* 260 (2015) 243.